Journal of the European Ceramic Society 20 (2000) 441–451

α-Silicon carbide/β-silicon carbide particulate composites via polymer infiltration and pyrolysis (PIP) processing using polymethylsilane☆

Mark A. Nechanicky [a,1], Kean W. Chew [a,1], Alan Sellinger [b], Richard M. Laine [a,*,1]

[a] *Department of Materials Science and Engineering, Chemistry, University of Michigan, Ann Arbor, MI 48109-2136, USA*
[b] *Macromolecular Science and Engineering Center, University of Michigan, Ann Arbor, MI 48109-2136, USA*

Received 3 March 1999; received in revised form 16 June 1999; accepted 28 June 1999

Abstract

The β-SiC precursor polymethylsilane [PMS, $[(MeSiH)_x,(MeSi)_y]]_n$. Mn = 2100 Da], when modified with 12 wt% crosslinking aid, gives a hyperbranched polymer (mPMS) that transforms to phase pure, nanocrystalline β-SiC with an 80–85% ceramic yield on heating to ≈1100°C/Ar. Particulate reinforced β-SiC composites (PRCs) can be formed by PIP processing green powder compacts. We describe here PIP processing of α-SiC/β-SiC PRCs using mPMS. The resulting composites have densities >2.5 g/cc (85% theory) after 10 PIP cycles. XRD and FTIR studies suggest that α-SiC seeds crystallization of mPMS derived β-SiC at temperatures ⩽1200°C.

Keywords: SiC; Composites; Precursors-organic; Polymethylsilane; Polymer infiltration

1. Introduction

Ceramic matrix composites (CMCs) encompass a diverse number of materials in terms of both chemical composition and physical morphology.[1–13] Most CMCs fall into two general categories: particulate (PRC) and fiber reinforced (FRC) materials, with numerous theoretical combinations of materials possible. Practically, however, the materials available for CMC fabrication impose physical limitations that reduce the number of CMC systems that have been studied.

For example, mismatches in coefficients of thermal expansion (CTE) magnify the inherent brittleness of ceramics as the strain resulting from CTE mismatches scales linearly with temperature. CTE mismatch can also cause premature fatigue failure, and for non-oxide CMCs, can cause spalling of protective layers in high temperature, oxidizing environments.[1,9] Chemical incompatibility may cause undesirable phases to form at matrix-reinforcement interfaces, affecting overall CMC mechanical properties.[14] Most ceramics are not wetted well by liquids and molten materials with high surface tension energies and low interfacial bond energies.[15,16] Thus, differences in intrinsic properties, processability, and phase purity requirements limit the number of materials that are compatible for CMC fabrication.

These concerns are compounded by processing variables that, taken together, contribute to process complexity, utility, cost, and commercial practicality. One solution to the above problems is to process CMCs of like materials, e.g. α-SiC/β-SiC so that problems of chemical incompatibility and CTE mismatch are avoided without diminishing final CMC utility or increasing processing costs.

Efforts to minimize CMC processing times and costs have led to the development of a wide range of fabrication methods that fall into four general categories.[1] The first category includes conventional powder processing, such as sintering and hot isotactic pressing methods, which provide dense ceramics and composites [17–19] but involve slow, expensive, and high temperature processing to obtain fully dense composites. Furthermore, only simple geometric shapes are accessible. A common

☆ Work supported by ARO through grant nos. DAAH04-95-1-0407 and DAAL03-92-G-0053, and by Lockheed Martin Corp.

* Corresponding author.
[1] Member, American Ceramic Society.

0955-2219/00/$ - see front matter
PII: S0955-2219(99)00177-6

problem associated with high temperature processing is that finished components often exhibit excessive grain growth and or reinforcement degradation as the high temperatures used promote matrix-reinforcement interfacial reactions.[1,2]

The second category includes reactive melt infiltration processes, e.g. infiltrating molten Si into microporous carbon preforms to produce SiC/Si composites.[20–25] Near net-shape, dense composites result, but the metal must wet the solid phase well as interfacial reactions greatly influence the processing speed, and final product properties.[26–28]

The third class is based on in situ techniques such as chemical vapour infiltration or deposition (CVI or CVD).[29–32] CVI processes often require high temperatures and pressures, leading to energy and equipment intensive processes. In addition, these processes often require the use of toxic/corrosive gases, which can be problematic.[37]

The last class is chemical processing via sol–gel or polymer precursor routes.[33–40] The advantages are lower average processing temperatures, effective atomic mixing of composite components and hence greater homogeneity, and the potential for forming multiphase matrices. In both methods, a liquid precursor form of the ceramic is infiltrated into a fiber or particle preform to introduce the matrix phase. The precursor is then converted typically by hydrolysis in sol–gel processing and by thermal decomposition in the polymer precursor method. The resulting matrix must be densified and then the process repeated several times before relatively dense matrices form.

The major disadvantages to sol–gel processing are low ceramic yields, high volume shrinkage, and slow gelation rates.[1] Also, since water is a frequent reactant, sol–gel approaches, typically are useful only for oxide precursors. The alternative, polymer precursor infiltration and pyrolysis or PIP processing of the matrix phase provides access to non-oxide matrices but also has its drawbacks. In particular, multiple PIP cycles are required to achieve reasonable matrix densities.

For PIP processing to be successful, three general parameters must be optimized:

1. precursor quality (high ceramic yield, phase and chemical purity upon pyrolysis, and controlled microstructural evolution);
2. porosity (minimal and completely open porosity in green compacts and during PIP cycling);
3. microstructure (controlled densification with minimal grain growth during sintering).[1,2,35]

These general parameters provide objectives for the work presented here on PIP processing of α-SiC/β-SiC PRCs using a β-SiC precursor. This work is an extension of research described by Chew et al.[35] on PIP processing of AlN/β-SiC PRCs using modified polymethylsilane (mPMS, described below).[35] In this earlier work, evidence indicates that the addition of 10 wt% submicron α-SiC powder to AlN powder compacts seeds and promotes β-SiC grain growth at $\geqslant 1000^{\circ}C$.

Based on these results, we sought to use seeding to promote low temperature crystallization and densification in PIP processed MC/β-SiC PRCs including α-SiC/β-SiC, B_4Cβ-SiC, TiCβ-SiC, H_fC/β-SiC, and ZrC/β-SiC. The work reported here emphasizes the α-SiC/β-SiC system, wherein α-SiC polytype particles are used as the reinforcing phase and the β-SiC matrix phase is derived from pyrolysis of an infiltrated mPMS.

2. Experimental

2.1. Materials

α-SiC powders were obtained from Cerac, Inc. (Milwaukee, W1). The reported particle sizes were <1 μm (fine, 99.9%, lot X19243-1) and 10–44 μm (coarse, 99%, lot X17218). The precursor mPMS is synthesized from reagent grade chemicals. The synthesis and characterization of mPMS is described briefly below and reported completely elsewhere.[35,40–43]

2.2. Analytical methods

2.2.1. Thermogravimetric analysis TGA

A Hi-Res TGA 2950 thermogravimetric analyzer (TA Instruments, Inc., New Castle, DE) was used to determine the ceramic yield of mPMS. Samples (≈25 mg) were placed in a platinum pan and heated in Ar (60 cc/min) at 50°C/min from 25 to 900°C. Sample mass losses were recorded over a period of 45 min.

2.2.2. Diffuse reflectance infrared Fourier transform (DRIFT)

A Mattson Galaxy Series Fourier transform infrared reflectance 3020 spectrometer (Mattson Instruments, Inc., Madison, WI) with dry N_2 purge was used to obtain spectra of pyrolysed mPMS and mPMS coated α-SiC powders. The coated powder specimens were prepared by mixing mPMS in toluene solution and α-SiC powder to give 1:1 wt:wt mPMS:SiC on vacuum drying. The coated powders were heated to 1000, 1200 and 1400°C/Ar/1 h. Samples of pyrolysed mPMS, as-received powders and coated α-SiC powders were made in the Ar dri-box by grinding with an alumina mortar and pestle a 1.0 wt% sample with random cuttings of optical grade KBr (International Crystal Laboratories, Garfield, NJ). The ground mixture was placed in an aluminum sample cup and moved into the specimen chamber. 500 scans were collected for each sample with a resolution of $\pm 4\ cm^{-1}$.

2.2.3. X-ray powder diffraction (XRD)

XRD patterns were used to determine the phases and degree of crystallinity of mPMS pyrolysed to 1000, 1200, and 1400°C/1 h/Ar (100 cc/min). Using standard methods, data were collected using a Rigaku Rotating Anode Goniometer (Rigaku Denki Company, Ltd., Tokyo, Japan).[43]

2.2.4. Transmission electron microscopy (TEM)

TEM (JOEL 2000 TM) characterization was performed on mPMS pyrolysed to 1000, 1200, and 1400°C/1 h/Ar (100 cc/min). The resulting β-SiC particles were ground in an alumina mortar and pestle, suspended in isopropanol, ultrasonicated, and pipetted onto a holey carbon TEM sample grid (SPI Inc.). After the isopropanol evaporated, the sample was analyzed using standard electron diffraction and bright/dark field magnification methods.[44] Diffraction patterns were obtained using a camera length of 100 cm. Dark field patterns were obtained by tilting the incident beam to align part of the {111} diffraction ring with the optic axis. The corresponding bright field was obtained by centering the direct beam.[45]

2.3. Powder preparation and compaction process

SiC PRC green discs (≈12 dia.×1 mm) were fabricated using a 1:1 (wt:wt) mixture (≈0.35 g) of fine and coarse α-SiC particles which were combined and mixed manually. A 1:1 (wt:wt) mixture compacts to the highest density (2 g/cc, ≈60 wt%) and exhibits the best green mechanical properties. Once formulated, the powder mixture was heated (20°C/min) to 1000°C/1 h/Ar to remove surface organics and adsorbed water before compaction.

The mixture was then coated with mPMS, which serves as a binder, by soaking the powder mixture with mPMS solution (25 wt% solids) in a clean, dry, soda-lime glass vial. The coated powder was then vacuum dried (36 h/25°C) and loaded into a 12.7 mm dia. double action tool steel die inside the Ar dri-box, removed from the Ar dri-box, and uniaxially compressed by gradual application of 100 MPa (Carver Laboratory Press) over 15 min. After removal from the die, discs were placed in alumina boats (52×30×13 mm) lined with graphite foil and heated using the schedule shown in Table 1. No die release agents/lubricants were used.

2.4. Pyrolysis conditions

All pyrolysis steps up to 1200°C were conducted in a silica glass tube (5.7 cm throat ID by 71.1 cm L) under Ar (100 cc/min) using a temperature programmable, single zone tube furnace (Lindberg model no. 55322-3; controller model no. 58114-P, Watertown, WI). Pyrolysis steps above 1200°C were carried out under Ar (100 cc/min) in a high temperature tube furnace (F54348CM, Barnstead/Thermolyne, Dubaque, IA) inside a sealed mullite tube equipped with a ported, water cooled, Al end cap.

Table 1
Heat treatment schedule for pyrolyzing impregnated PRCs

Heating ramp rate (°C/min)	Dwell temperature (°C)	Dwell time (h)
2.0	100	0.5
4.0	200	0.5
4.0	250	0.0
4.0	350	0.5
5.0	470	0.5
5.0	550	0.5
10.0	1000/1200/1400	1.0
10.0	23	End

2.5. Infiltration

Following the first heat treatment, the discs were transferred into the Ar dri-box. Sample masses and dimensions (≈12 dia.×1 mm) were recorded. The samples were then subjected to the first PIP cycle.

For each PIP cycle, individual discs were placed in clean, dry, soda-lime glass vials (14 mm dia.). Then, mPMS solution (≈5 ml, 10 wt% mPMS in toluene solution) was added by pipette until the entire disc was fully submerged. The discs were left in solution >12 h, then removed, dried and heat-treated to 1000°C. Each disc was subjected to ten PIP cycles.

When additional PIP cycles showed no further mass gains, a single 1200°C cycle was used to reopen pores in the PRC. This step permitted additional infiltration of mPMS throughout the PRC and processing at 1000°C. For the final processing step, the disc was first taken to 1200°C in a ported silica furnace tube and then taken to 1400°C inside a sealed mullite tube equipped with a ported, water cooled, Al end cap.

2.6. CMC characterization

2.6.1. Density measurements

Following pyrolysis as described above, the disc dimensions and weight were noted with digital calipers (CD-6'' C, Mitutoyo Corp., Japan) and a Mettler balance (PJ360 DeltaRange®, Highstown, NJ). The densities were calculated from these measurements.

2.6.2. Scanning electron microscope (SEM)

A 5 kV optimized-tungsten-gun SEM (Model S-3200N, Hitachi, Ltd., Tokyo, Japan) was used to image the processed PRCs. Sample cross-sections were cut using a high speed diamond wafer saw (Buehler Isomet 2000 Precision Saw, Buehler Ltd., Lake Bluff, IL). Specimen surfaces were polished with 1000 grit SiC paper and ultrasonically cleaned in water.

2.6.3. Lineal intercept fraction analysis

Lineal intercept fraction analysis was used to determine the porosity in a processed α-SiC/β-SiC PRC. The fraction of lines intersecting pores was measured from 84 lines over the entire cross-sectional area.

2.6.4. X-ray diffraction analysis

XRD was used to determine the crystalline phases and grain sizes obtained after samples were pyrolysed to 1000, 1200, and 1400°C for 1 h. PRC discs were placed in Al sample holders with the PRC surface flush with the sample holder surface. Spectra were collected using a Rigaku Rotating Anode Goniometer (Rigaku Denki Company, Ltd., Tokyo, Japan) using standard data acquisition methods.[44]

3. Results and discussion

Chew et al. recently reported that adding 10 wt% α-SiC powder to AlN green powder compacts significantly improves mPMS PIP processing of AlN/β-SiC PRCs. The added α-SiC seeds crystallization and grain growth of β-SiC during pyrolysis of mPMS at temperatures as low as 1000°C.[35] If seeded grain growth of mPMS can be promoted effectively, then densities approaching that of theory may be obtainable at processing temperatures $\leqslant$1200°C. Rather than the typical temperatures ($\geqslant$1800°C) required for full densification. This paper extends the Chew et al. work to mPMS PIP processing of α-SiC/β-SiC PRCs.

Initial studies on the α-SiC/β-SiC system focused on learning to make mechanically strong green compacts. In these studies it was found that a 1:1 (wt:wt, $<$1 μm:10–44 μm) bimodal mixture of α-SiC powders provided the highest green compact densities (2 g/cc ≈60 wt%).[35] PRC discs made with α-SiC powders coated with 25 wt% mPMS[46] binder had only slightly higher green densities than discs made without mPMS binder, but were significantly stronger and more easily handled. Discs were compacted in a double action stainless steel die to a maximum pressure of 100 MPa over a period of 15 min. Single action dies and pressures above 100 MPa produced compaction flaws in the PRC discs such as end capping and delamination. No sintering of the α-SiC/β-SiC discs was observed at temperatures $\leqslant$1400°C. The next step was to characterize the mPMS transformation process.

3.1. mPMS characterization

We have previously described a polymethylsilane (PMS) polymer precursor to β-SiC that makes PIP processing of α-SiC/β-SiC CMCs practical.[35,42] The addition of 12 wt% tris(trivinylsilylethyl)borane (TVS-B), a crosslinking and sintering aid, provides a modified version, mPMS, which can be used for: fiber processing;[47–49] joining;[50] and for PIP processing of pRCs and FRCs.[35,51]

The mPMS is prepared by first polymerizing either methylsilane[42,43] or methyldichlorosilane using sodium[35] and subsequently crosslinking with TVS-B. The idealized mPMS unit and pyrolysis products are given by:

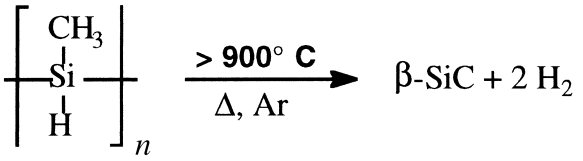

As prepared, mPMS is a toluene soluble solid with a number average molecular weight of ≈2100 Da, a polydispersity index of ≈7.1, and a composition $\approx C_{1.40}Si_{1.00}B_{0.02}$.[42,43] Excess C is deliberately added as TVS-B to ensure carbothermal removal of surface oxygen on the high surface area reinforcing particles. On heating to 1080°C/Ar, mPMS converts to phase pure, nanocrystalline ($<$50 nm) β-SiC with a 1:1 Si:C stoichiometry.[42,43] Heating mPMS to 1800°C provides high density ($>$3.1 g/cc), and nanocrystalline β-SiC with ave. grain sizes of 0.2–0.5 μm.[51] Note that the density at 1200°C is 2.4–2.5 g/cc as determined for SiC fibers.[47,48] The experimental ceramic yields are $>$80%. The complete synthesis of mPMS and its pyrolysis behaviour are described elsewhere.[35,42]

3.1.1. TGA

The theoretical β-SiC ceramic yield for PMS is 91%. TGA analysis of vacuum-dried mPMS shows a ceramic yield of ≈85% at 1000°C. The lower experimental ceramic yield is due to the loss of volatile, low molecular weight mPMS cyclomers (2.5 wt% at 250°C). The majority of the mass loss occurs gradually between 250 and 800°C due to methane and hydrogen losses. Additional hydrogen losses between 800 and 1450°C further reduce the experimental ceramic yield by 2–3 wt%.[35]

3.1.2. XRD

Complete XRD analyses of mPMS derived β-SiC are reported elsewhere.[35,42,43] The Fig. 1 XRDs show the evolution of peaks [(111, 35.60°, 4.73°; 2θ full width at half maximum intensity (FWHM), (220, 59.98°, 3.30°; 2θ FWHM), and (311, 71.77°, 2.28°; 2θ FWHM)] as mPMS is heated to 1000, 1200 and 1400°C. All of the XRDs consist of very broad, moderately intense β-SiC peaks indicative of nanocrystallinity. For samples heated to 1200 and 1400°C, the peaks sharpened slightly indicating some grain growth, but the 1400°C β-SiC remains nanocrystalline. Debye–Scherrer analyses of the highest intensity (111) peak at FWHM show grain sizes of ≈2 nm (1000°C), ≈3 nm (1200°C), and ≈4 nm (1400°C). As detailed elsewhere, the resulting nanocrystalline materials are dense and phase pure,[35,42,43] thus

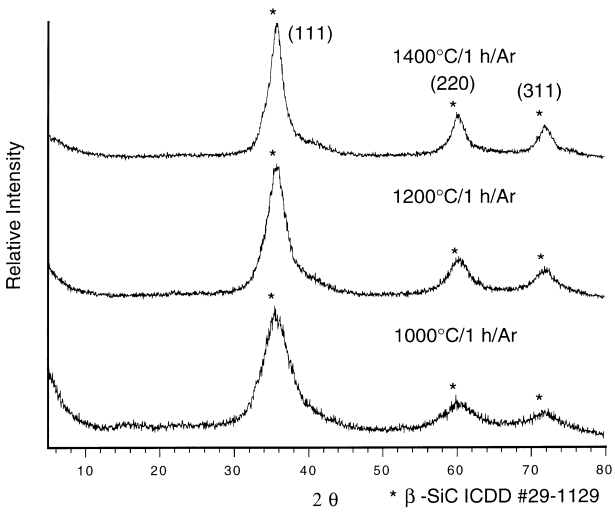

Fig. 1. XRD of mPMS pyrolysed to 1000, 1200 and 1400°C/1 h/Ar indicating nanocrystalline grains.

satisfying the first general processing parameter discussed above.

3.1.3. DRIFT spectra

DRIFT spectroscopy is very sensitive to sample crystallinity, particle size, and bond type; the higher the degree of crystallinity (larger the grain size) the sharper the peaks are in the IR.[50] DRIFTS of mPMS pyrolysed to 1000, 1200, and 1400°C are presented in Fig. 2. They show broad peaks at 900 and 780 cm^{-1} typical of SiC stretching vibrations, but also typical of nanocrystalline material, in keeping with the XRD data above.[35,42,43] Some peak sharpening appears to occur as mPMS is pyrolysed to 1200 and 1400°C corroborating XRD data showing limited grain growth (Fig. 1). In contrast, DRIFT spectra (see below) of fine α-SiC powders (Cerac) and β-SiC (Cerac) are indistinguishable and show a sharp, primary peak at 900 cm^{-1}.

3.1.4. TEM

Fig. 3 shows bright and dark field images of the mPMS derived monolithic β-SiC pyrolysed to 1000°C. A measured grain size of $\leqslant$10 nm was determined from magnified dark field micrographs. The white grains seen in the dark field correspond to the {111} planes of the cubic β-SiC electron diffraction pattern shown in Fig. 4 (ICDD No. 29-1129). More precise data obtained from HR-TEM studies of mPMS derived β-SiC fibers heated to selected temperatures give grain sizes ≈1 nm (1000°C), 10 nm (1200°C), and 25 nm (1400°).[42,43,53]

3.2. Polymer infiltration and pyrolysis (PIP) processing

3.2.1. mPMS infiltration

The mPMS solution, as produced, contains ≈10 wt% mPMS. Related studies[35] indicate that increasing the mPMS concentration does not significantly increase

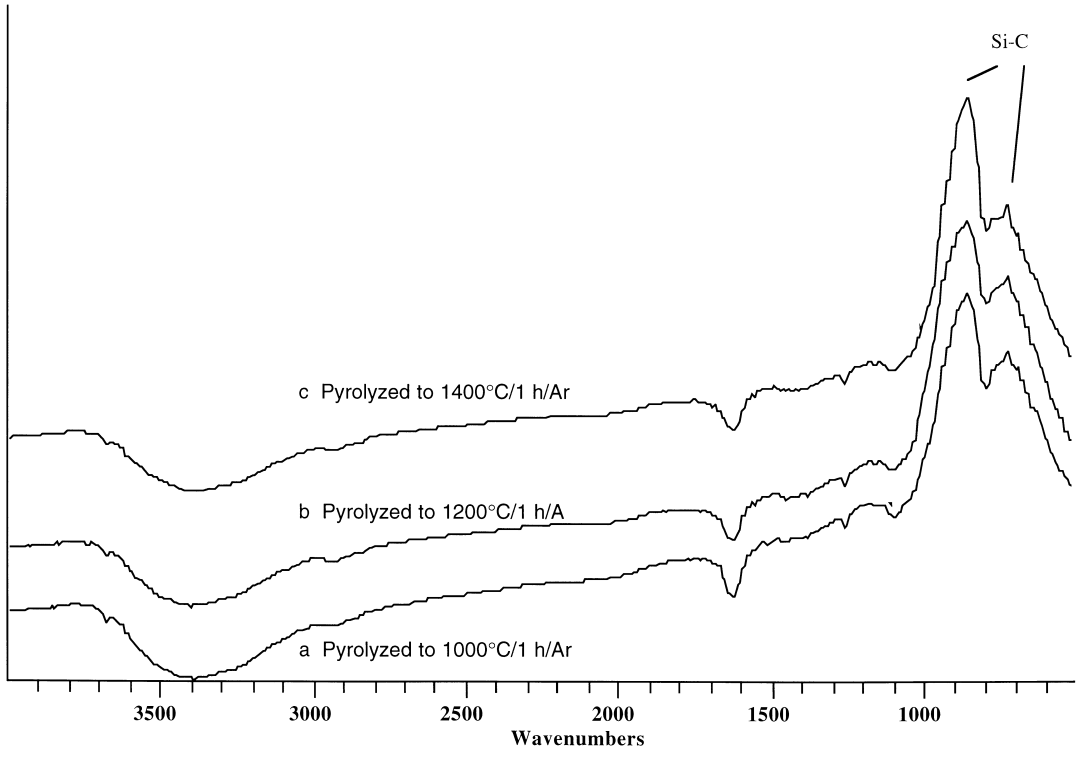

Fig. 2. Diffuse reflectance FTIR of mPMS pyrolysed to 1000, 1200 and 1400°C/1 h/Ar.

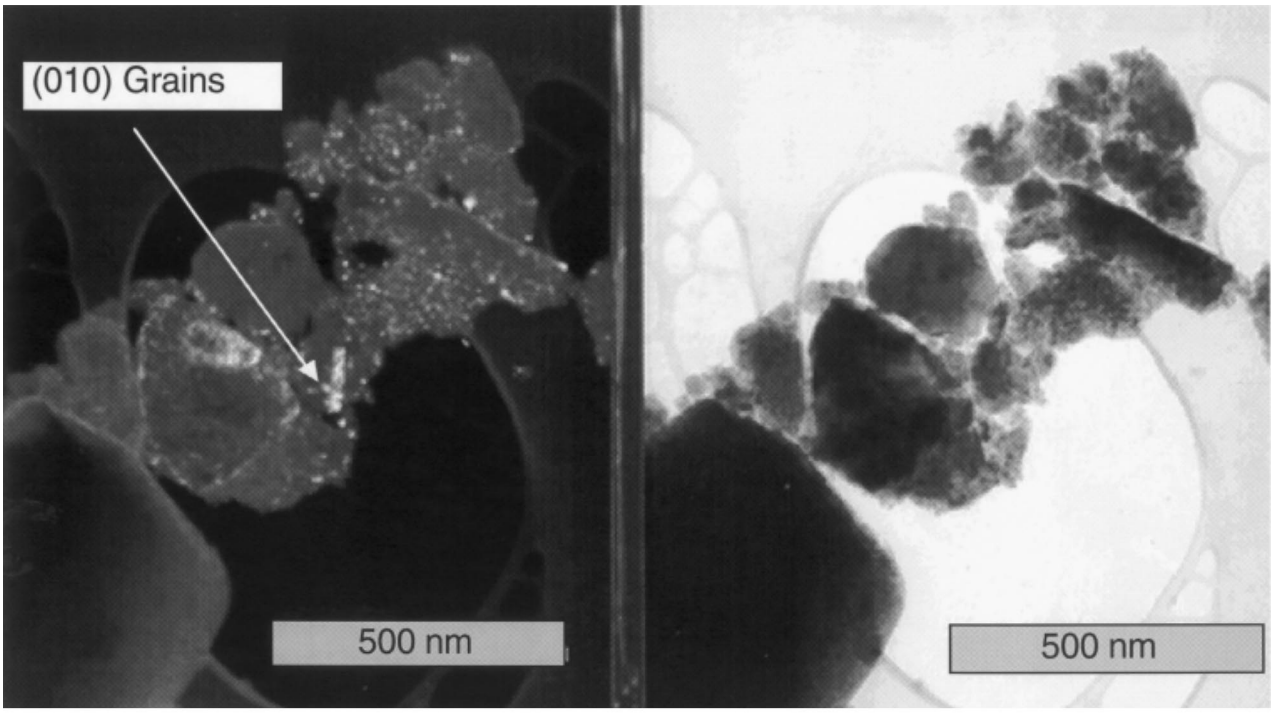

Fig. 3. Dark field/bright field TEMs of bulk β-SiC obtained from mPMS pyrolysed to 1000°C/1 h/Ar showing 10–50 nm grains.

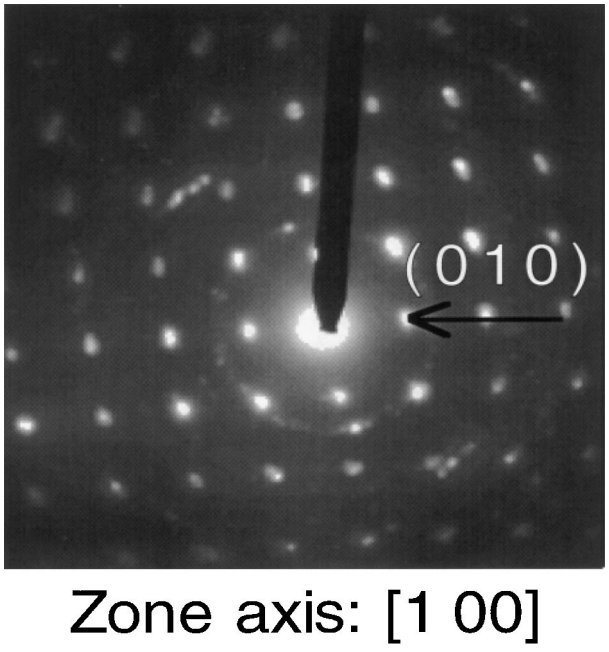

Fig. 4. Electron diffraction pattern corresponding to the (010) β-SiC grains in Fig. 3.

the amount of precursor infiltrated into the compact. Infiltration times of ≈12 h were used for all PIP cycles to allow for the maximum amount of precursor to infiltrate into the compact via capillary action. For infiltration periods beyond 12 h, no bubbles were observed leaving the compact, signifying that infiltration was complete. No effort was made to minimize infiltration times.

3.2.2. *Pyloilsis steps and furnace schedules*

The pyrolysis heat treatment schedule was established based on the mPMS TGA profile.[35] The pyrolysis rate was controlled such that a constant mass loss was achieved over the entire schedule to avoid excessive outgassing that might damage the discs. The heat treatment schedule used is shown in Table 1.[35] Again, no efforts were made to optimize this schedule.

All processing was conducted using a preset 10 PIP cycle limit. This arbitrary choice is mandated by the fact that PIP methods becomes considerably less attractive with increasing numbers of PIP cycles. The majority of the pyrolysis steps were performed at 1000°C; however after ≈5 PIP cycles, no further weight gains were observed. Thus, a single PIP cycle to 1200°C was run to further densify the β-SiC matrix and reopen the pores throughout the compact. This permitted weight gains with additional PIP cycles at 1000°C.[35]

Samples were heat treated at 1400°C/1 h/Ar when no further weight gains were observed even after a 1200°C PIP cycle. Sample densities were unchanged by the 1400°C treatment (as discussed below).

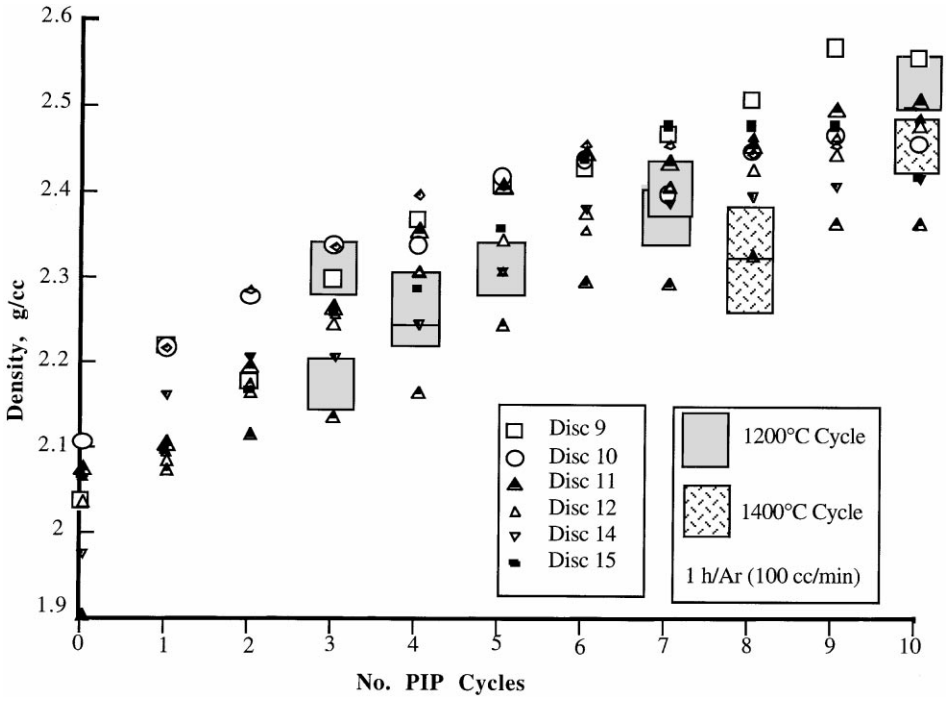

Fig. 5. Density improvements in α-SiC/β-SiC PRCs with PIP cycles.

3.3. PRC characterization

3.3.1. PRC density improvements

Fig. 5 shows the density improvements of PRC discs with increasing numbers of PIP cycles. Within 10 PIP cycles, PRC densities $\leqslant$2.55 g/cc were obtained from initial green densities of 2.1 g/cc with 25 wt% mPMS binder without going above 1400°C.

The density of β-SiC derived from mPMS in the α-SiC/β-SiC PRCs processed to 1200°C was calculated to be 2.5 g/cc from the rule of mixtures:

$$\rho_c = V_{\alpha-\mathrm{SiC}}\rho_{\alpha-\mathrm{SiC}} + V_{\beta-\mathrm{SiC}}\rho_{\beta-\mathrm{Si}}$$

where ρ_c, $V_{\alpha-\mathrm{SiC}}$, $V_{\beta-\mathrm{SiC}}$, $\rho_{\alpha-\mathrm{SiC}}$, $\rho_{\beta-\mathrm{SiC}}$ are the composite density (2.55 g/cc), volume fractions of the α-SiC and β-SiC phases, and densities of the α-SiC and β-SiC phases, respectively. The density of α-SiC is 3.19 g/cc. From the SEM studies below, we find that the porosity for this sample is about 10 vol%. The volume fraction of α-SiC and β-SiC are 50% (green compact density w/o mPMS binder, ≈1.6 g/cc) and 40%, respectively. Thus, one can calculate that the density of mPMS derived β-SiC at 1200°C is ≈2.4 g/cc. This is similar to 1200°C β-SiC density measurements from β-SiC fibers synthesized using mPMS (2.5 g/cc).[42,43,47,48] The achieved densities of 2.55 g/cc are >90% of the rule of mixtures theory (≈2.80 g/cc).

3.3.2. SEM

The Fig. 6 micrograph shows a cross section of an α-SiC/β-SiC PRC after 10 PIP cycles and a maximum processing temperature of 1400°C. The cross-section reveals uniform 5–25 μm pores throughout the entire cross-section indicating that the precursor infiltrates uniformly to the center of the PRC. Lineal intercept analysis indicates 9% porosity. Unfortunately, these pore sizes suggest that at the current stage of development, good mechanical properties are not obtained; although better infiltration (e.g. under vacuum) and higher final heat treatments may alleviate this problem.

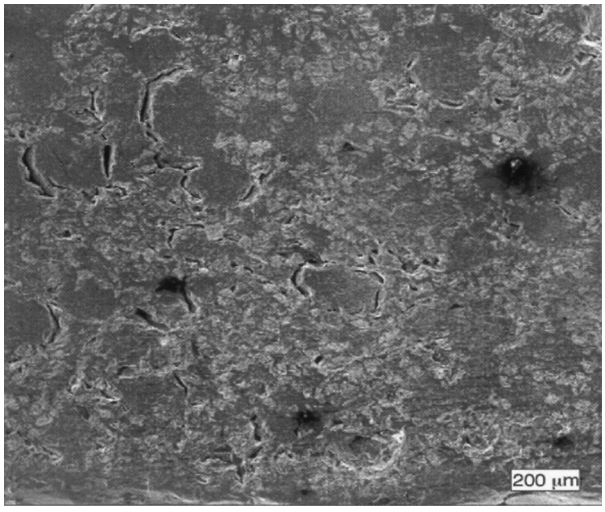

Fig. 6. SEM of cross-section of a α-SiC/β-SiC PRC showing a uniform porosity of 9%.

3.3.3. XRD

Previous studies of β-SiC fibers derived from mPMS, the above studies on pyrolysed bulk mPMS (Fig. 1), and

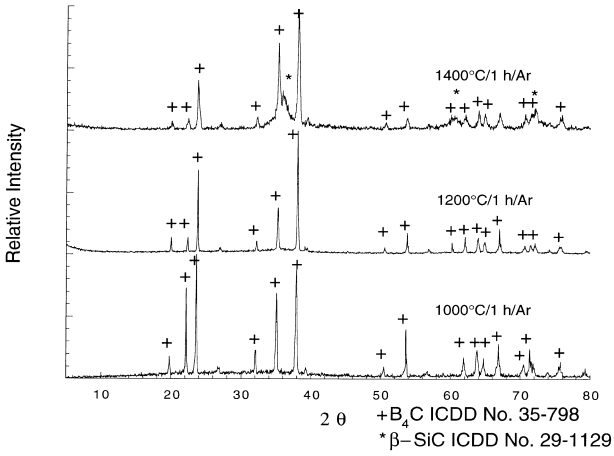

Fig. 7. XRD of B_4C/β–SiC PRC indicating that the β-SiC grain growth is not seeded.

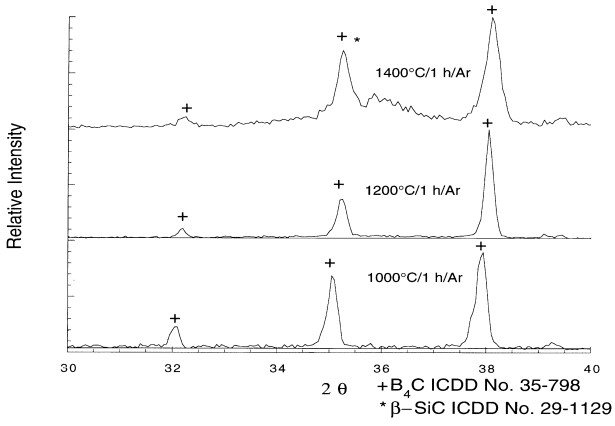

Fig. 8. 30–40° 2Θ region of B_4C/β-SiC PRC of Fig. 7.

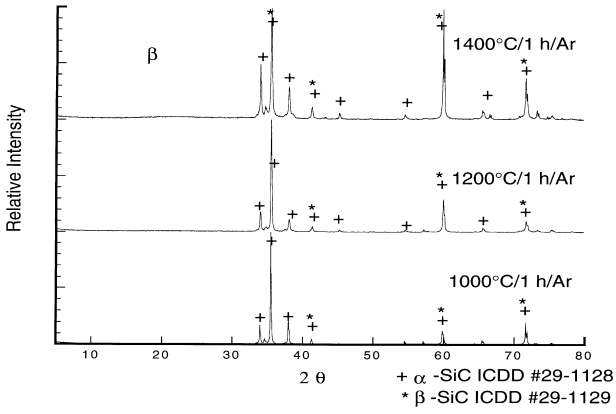

Fig. 9. XRD of the α-SiC/β-SiC PRC.

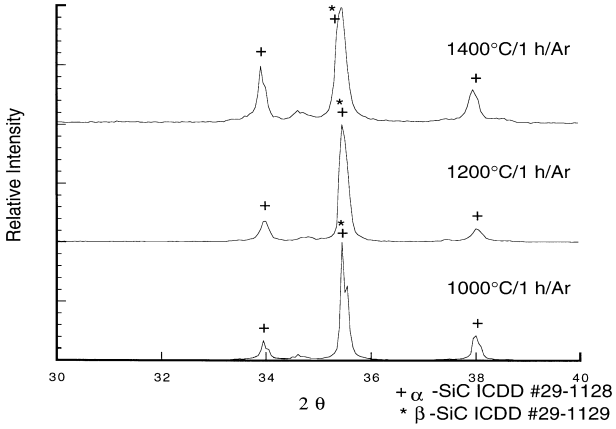

Fig. 10. 30–40° 2Θ region of α-SiC/β-SiC PRC of Fig. 9.

additional PIP studies of B_4C/β-SiC PRCs using mPMS[51] show broad β-SiC XRD peaks (Figs. 7 and 8, underlying the sharp B_4C powder pattern) after processing to 1400°C. These results are all consistent with limited β-SiC grain growth. In contrast, Figs. 9 and 10 show no evidence of the typically broad β-SiC Peaks seen in Figs. 1, 7 or 8. Only sharp lines typical of well-crystallized SiC are seen, suggesting that α-SiC seeds grain growth of the polymer derived β-SiC.[51]

XRD analysis of processed α-SiC/β-SiC PRCs is difficult due to the extensive overlap between the powder patterns of the hexagonal α-SiC phase and the cubic β-SiC phase. As shown in Table 2, all six of the first β-SiC peaks overlap with α-SiC peaks. The (101) α-SiC peak is used to determine the presence of the α-SiC phase. Figs. 8 and 10 provide expanded XRD plots (from 30 to 40°) of both the B_4C/β-SiC and α-SiC/β-SiC PRCs. Fig. 8 contains a very broad 102 peak at 35.60°2θ not seen in Fig. 10; although sharp peaks for α-SiC (101, 34.09°), (102, 35.66°), (103, 38.15°), (104, 41.40°), (105, 45.32°)

Table 2
List of prominent/common XRD peak positions for α-SiC and β-SiC

Compound	Intensity (relative)	hkl	2θ
α-SiC	35	101	34.09
	100	102	35.66
	35	103	38.15
	14	104	41.40
	5	105	45.32
	6	107	54.68
	43	110	59.99
	12	109	65.71
	2	201	70.84
	28	202	73.35
	4	203	75.51
	3	204	89.99
β-SiC	100	111	35.60
	20	200	41.38
	35	220	59.98
	25	311	71.77
	5	222	75.49
	5	400	90.00

peaks and relatively sharp (111, 35.60°), (200,41.38°) β-SiC peaks are observed with no obvious broadening. However, using these data to imply seeding of crystallization is insufficient. Thus, we turned to DRIFTS for further substantiation.

3.3.4. DRIFT

Spectra of free flowing α-SiC powder coated with 50 wt% mPMS (1:1 wt:wt ratio) heated to 1000, 1200, and 1400°C/Ar/1 h are shown in Fig. 11. Rather than the broad peaks seen in Fig. 2, only a sharp peak is observed at 900 cm^{-1} again suggesting that the β-SiC derived from mPMS has experienced grain growth. This corroborates the XRD data above.

Although some SiC precursors crystallize on heating to temperatures $\leqslant$750°C/2 h[52] mPMS does not normally convert to β-SiC until $>$900°C/2 h and the resulting grains are always nanocrystalline ($<$50 nm). Larger (0.3–0.5 μm) grains and nearly full densification do not normally occur until $\geqslant$1800°C.[42,51] Recent work by Heimann et al.[54] and Chew et al.[35] however, shows that precursor derived β-SiC grain growth occurs with α-SiC seeds. Heimann et al. grew single crystal thin films of β-SiC on α-SiC single crystals using a polyvinyImethylsilane precursor. After dipcoating the precursor onto the substrate, an amorphous β-SiC thin film (200 nm) developed on processing to 1100°C/Ar which then converted to epitaxial β-SiC at 1600°C/10 h/N_2. Chew et al. find that a 10 wt% addition of α-SiC powders to AlN powder compacts seeds grain growth of β-SiC at temperatures $\leqslant$1200°C.

Since the SiC/β-SiC system described uses the same precursor and α-SiC powders as the AlN/SiC system reported by Chew et al., and based on the work of Heimann et al. there is a strong possibility that seeded epitaxial grain growth occurs in the α-SiC/β-SiC system reported here. Additional support for this conclusion is found by contrasting the XRD from the α-SiC/β-SiC system with the XRD of the B_4C/β-SiC system which show sharp and broad XRD peaks, respectively. Full proof of epitaxial growth must await further TEM studies, but the work done to date suggests the possibility of PIP processing dense β-SiC matrices at lower temperatures.

The one key question that remains to be answered is why the densities of the polymer-derived β-SiC are not higher. Although we have no detailed explanation, we know that considerable hydrogen remains (2–3 wt%) within the mPMS derived β-SiC at 1200°C and this is likely the cause of the lower than expected densities. The only difference may be that instead of being homogeneously dispersed, seeding may force or promote hydrogen transport to the grain boundaries. More work will have to be done to prove or disprove this supposition.

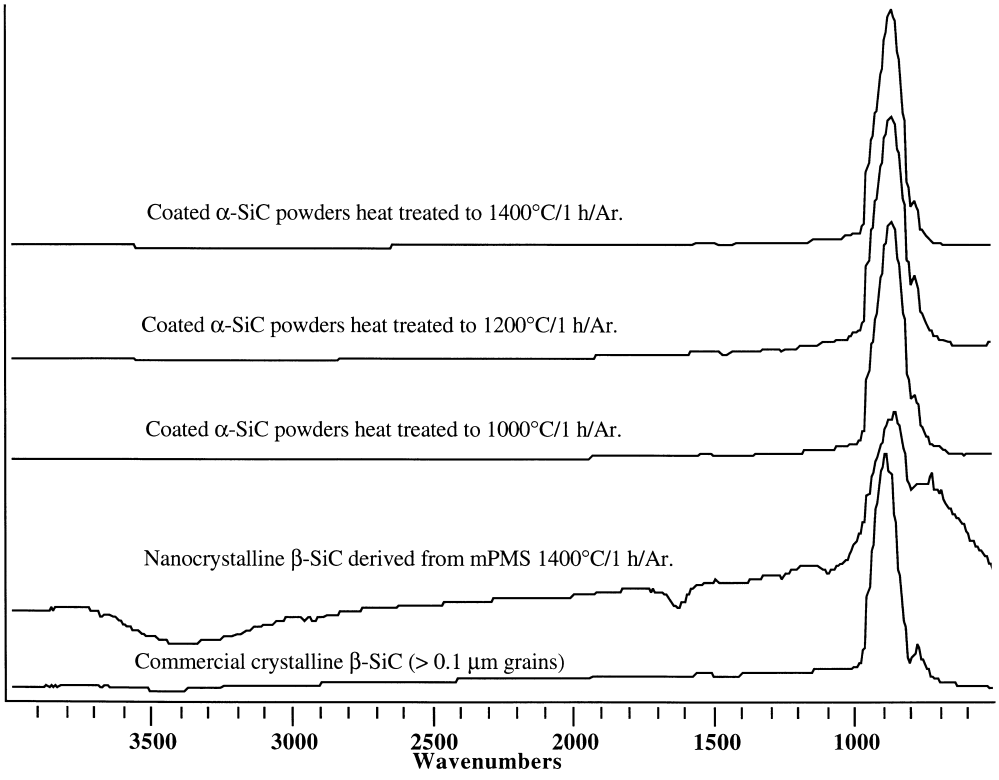

Fig. 11. Diffuse reflectance FTIRs of seeded and unseeded mPMS heated to selected temperatures.

4. Conclusions

PIP processing of α-SiC/β-SiC CMCs was studied using mPMS, a precursor to β-SiC. The matrix phase derived from mPMS increased the densities of α-SiC/β-SiC CMCs from 2.0 g/cc to 2.5 ± 0.05 g/cc which is $90 \pm 2\%$ of theory. The results suggest that the β-SiC grain growth is seeded by the α-SiC polycrystals from the reinforcement phase as seen by Chew et al. and Heimann et al. If β-SiC grain growth is seeded, we should be able to process all of the composites at 1000–1200°C, approach theoretical densities, and achieve full densification by using a final, short processing step of 1800°C. This important result coupled with the high ceramic yield of mPMS means we may be able to produce dense α-SiC/β-SiC PRCs and CMCs, with a limited number of PIP cycles and perform the majority of steps at low temperatures, saving time, energy, and equipment wear.

References

1. Cornie, J. A., Chiang, Y. M., Uhlmann, D. R., Mortensen, A. and Collins, J. M., Processing of metal and ceramic matrix composites. *Am Ceram. Soc. Bull.*, 1986, **65**(2), 293–296.
2. Schioler, L. J. and Stiglich Jr, J. J., Ceramic matrix composites: a literature review. *Am Ceram. Soc. Bull.*, 1986, **65**(2), 289–292.
3. Kostopoulous, V., Vellios, L. and Pappas, Y. Z., Fatigue behaviour of 3-d SiC/SiC composites. *J. Mater. Sci.*, 1997, **32**(1), 215–220.
4. Ueno, K. and Takahiro, I., Preparation and properties of SiC fiber reinforced SiAlON ceramic composite. *Ceram. Inter.*, 1997, **23**(2), 165–170.
5. Lackey, W. J., Vaidyaraman, S. and More, K. L., Laminated C-SiC matrix composites produced by CVI. *J. Am. Ceram. Soc.*, 1997, **80**(1), 113–116 .
6. Lin, P. K. and Tsai, D. S., Preparation and analysis of a silicon carbide composite membrane. *J. Am Ceram. Soc.*, 1997, **80**(2), 365–372.
7. Singh, M., Dickerson, R. M., Olmstead, F. A. and Eldridge, J. I., SiC (SCS-6) fiber reinforced reaction formed SiC matrix composites: microstructure and interfacial properties. *J. Mater. Res.*, 1997, **12**(3), 706–713.
8. Pluvinage, P., Parvizi-Majidi, A. and Chou, T. W., Damage characterization of two-dimensional woven and three-dimensional braided SiC-SiC composites. *J. Mater. Sci.*, 1996, **31**(1), 232–241.
9. Fitzer, E. and Gadow, R., Fiber reinforced silicon carbide. *Am. Ceram. Soc. Bull.*, 1986, **65**, 326–335.
10. Lamicq, P. L., Bernhart, G. A., Dauchier, M. M. and Mace, J. G., SiC/SiC composite ceramics. *Am. Ceram. Soc. Bull.*, 1986, **65**, 336–338.
11. Stinton, D. P., Caputo, A. J. and Lowden, R. A., Synthesis of fiber-reinforced SiC composites by chemical vapor infiltration. *Am. Ceram. Soc. Bull.*, 1986, **65**, 347–350.
12. Riedel, R., Strecker, K. and Petzow, G., In situ polysilane-derived silicon carbide particulates dispersed in silicon nitride composites. *J. Am. Ceram. Soc.*, 1989, **72**(11), 2071–2077.
13. Whitehead, A. J. and Page, T. F., Fabrication and characterization of some novel reaction bonded silicon carbide materials. *J. Mater. Sci.*, 1992, **27**(3), 839–852.
14. Gao, Y., Jia, J., Loehman, R. E., Ewsuk, K. G. and Fahrenholtz, W. G., Microstructure and composition of Al-Al_2O_3 composites made by reactive metal penetration. *J. Mater. Sci.*, 1996, **31**(15), 4025–4032.
15. Nicholas, M. G., Reactive metal brazing of ceramics. *Scand. J. of Metal.*, 1991, **20**(2), 157–164.
16. Long, S., Zhang, Z. and Flower, H. M., Characterization of liquid metal infiltration of a chopped fiber preform aided by external pressure–I. Visulization of the flow behavior of aluminum melt in a fiber preform. *Acta. Metall. Mater.*, 1995, **43**(9), 3489–3498.
17. Brenan, J. J. and Prewo, K. M., Silicon carbide fiber reinforced glass-ceramic matrix composites exhibiting high strength and toughness. *J. Mater. Sci.*, 1982, **17**(8), 2371–2383.
18. Sambell, R. A. J., Briggs, A. and Phillips, D. C., Carbon fiber composites with ceramic and glass matrices, Part 1 — discontinuous fibers. *J. Mater. Sci.*, 1972, **7**(6), 663–675.
19. Sambell, R. A. J., Briggs, A. and Phillips, D. C., Carbon fiber composites with ceramic and glass matrices, Part 2 — continuous fibers. *J. Mater. Sci.*, 1972, **7**(6), 676–681.
20. Hozer, L., Lee, J. R. and Chiang, Y. M., Reaction infiltrated, net-shape SiC composites. *Mat. Sci. Eng. A*, 1995, **A195**(1–2), 131–143.
21. Behrendt, D. R. and Singh, M., Effect of carbon preform pore volume and infiltrants on the composition of reaction-formed silicon carbide materials. *J. Mater. Syn. and Proc.*, 1994, **2**(2), 117–123.
22. Rosenlocher, J., Feldmann, M. and Greil, P., Non-oxide CMC formation by reactive melt infiltration. *Key Eng. Mater.*, 1997, **132–136**, 1882–1885.
23. Singh, M. and Behrendt, D. R., Reactive melt infiltration of silicon-niobium alloys in microporous carbons. *J. Mater. Res.*, 1994, **9**(71), 1701–1708.
24. Loeliman, R. E., Ewsuk, K. and Tomasi, A. P., Synthesis of Al_20_3-Al composites by reactive metal infiltration. *J. Am Ceram Soc.*, 1996, **79**(1), 27–32.
25. Lange, F. F., Velamakanni, B. V. and Evans, A. G., Method for processing metal-reinforced ceramic composites. *J. Am. Ceram. Soc.*, 1990, **73**(2), 388–393.
26. Delannay, F., Froyen, L. and Deruyttere, A., Review: the wetting of solids by molten metals and its relation to the preparation of metal-matrix composites. *J. Mater. Sci.*, 1987, **22**, 1–16.
27. Li, J. G., Vetting of ceramic materials by liquid silicon, aluminum and metallic melts containing titanium and other reactive elements: a review. *Ceram. Inter.*, 1994, **20**(6), 391–412.
28. Aksay, I. A., Hoge, C. E. and Pask, L. A., Wetting under chemical equilibrium and nonequilibrium conditions. *J. Phys. Chem.*, 1974, **78**(12), 1178–1183.
29. Day, P. S., Skamser, D. J., Faber, K. T., Jennings, H. M. and Johnson, D. L., Damage tolerance of silicon carbide- and alumina-matrix surface composites. *J. Am Ceram. Soc.*, 1996, **79**(4), 1117–1120.
30. Morell, J. I., Economou, D. J. and Amundson, N. R., Chemical vapor infiltration of SiC with microwave heating. *J. Mater. Res.*, 1993, **8**(5), 1057–1067.
31. Naslain, R., Two-dimensional SiC/SiC composites processed according to the isobaric-isothermal chemical vapor infiltration gas phase route. *J. Alloys and Comps.*, 1992, **188**(1–2), 42–48.
32. Bansal, N. P., CVD SiC fiber-reinforced barium aluminosilicate glass-ceramic matrix composite. *Mater. Sci. Eng. A*, 1996, **A**(220,1–2), 129–139.
33. Raman, V., Bahl, O. P. and Dhawan, U., Synthesis of silicon carbide incorporated carbon–carbon composites by sol-gel process. *J. Mater. Sci. Lett.*, 1995, **14**(16), 1150–1152.
34. Lee, B. I. and Park, S-Y., Sol–gel processing of SiC-whisker-reinforced silica-based ceramic composites. *J. Am Ceram. Soc.*, 1989, **72**(12), 2381–2385.

35. Chew, K. W., Sellinger, A. and Laine, R. M., Processing of aluminum, nitride/silicon carbide composites via polymer infiltration and pyrolysis of polymethylsilane, a precursor to stoichiometric SiC. *J. Am. Ceram. Soc*., 1999, **82**, 857–866.
36. Tu, W. C. and Lange, F. E., Liquid precursor infiltration processing of powder compacts: I, kinetic studies and microstructure development. *J. Am. Ceram. Soc*., 1995, **78**(12), 3277–3288.
37. Interrante, L. V., Whitinarsh, C. W. and Sherwood, W., Tabrication of SiC matrix composites by liquid phase infiltration with a polymeric precursor. *Mat. Res. Soc. Symp. Proc*., 1995, **365**, 139–146.
38. Mayer, J., Szabo, D. V., Ruehle, M., Seher, M. and Reidel, R., Polymer-derived Si-based bulk ceramics, Part II: microstructural and characterizational by electron spectroscopic imaging. *J. Eur. Ceram. Soc*., 1995, **15**(8), 717–727.
39. Hinklin, T., Neo, S. S., Chew, K. W., Laine, R. M. Precursor impregnation and pyrolysis (PIP) processing of barium/strontium aluminosilicate-nicalon composites. to be submitted.
40. Laine, R. M. and Babonneau, F., Preceramic routes to silicon carbide. *Chem. Mater*., 1993, **5**, 260–279.
41. Baney, R. H., Gaul, J. H. and Hilty, T. K., Methylchloropolysilanes and derivatives prepared from the redistribution of methylchlorodisilanes. *Organometallics*, 1993, **2**, 859–863.
42. Zhang, Z. F., Scotto, C. S. and Laine, R. M., Processing stoichiometric silicon carbide fibers from polymethylsilane. I. Precursor fiber processing. *J. Mater. Chem*., 1999, **8**, 2715–2724.
43. Laine, R. M. and Sellinger, A. Si-containing ceramic precursors. In: *The Chemistry of Organic Silicon Compounds*, Vol. 2, eds Z. Rappaport and Y. Apeloig. John Wiley and Sons, London, 1998, pp. 2245–2310.
44. Cullity, B. D. In Elements of X-ray Diffraction, Addison-Wesley Pub. Co. Inc., Reading, MA, 1978.
45. Eddington, J. W. In Practical Electron Microscopy in Materials Science, TechBooks, Herndon, VA, 1976.
46. Schwartz, K. B. and Rowcliffe, D. J., Modeling density contributions in preceramic polymer/ceramic powder systems. *J. Am Ceram. Soc*, 1986, **69**, C106.
47. Zhang, Z. F., Scotto, C. S. and Laine, R. M., Pure silicon carbide fibers from polymethylsilane. *Ceram. Eng. Sci. Proc*., 1994, **15**, 152–161.
48. Zhang, Z. F., Scotto, C. S. and Laine, R. M., Processing stoichiometric silicon carbide fibers from polymethylsilane. Part 1. Precursor fiber processing. *J. Mater. Chem*., 1998, **8**, 2715–2724
49. Zhang, Z. F., Kennish, R. A., Youngdahl Blohowiak, K. A., Hoppe, M. L. and Laine, R. M., Superconducting fibers from organometallic precursors: Part III. Pyrolytic processing of precursor fibers. *J. Mater. Res*., 1993, **8**(8), 1777–1790.
50. Treadwell, D. R., Laine, R. M., Burzynski, R. Joining of SiC monoliths with polymethylsilane. *J. Am. Ceram. Soc*. to be revised
51. Nechanicky, M. A., Chew, K., Narayanan, R., Laine, R. M. B_4C/SiC particulate composites via polymer infiltration and pyrolysis of polymethylsilane, unpublished work
52. Liu, Y., Zhang, Z. F., King, B., Halloran, J. and Laine, R. M., Synthesis of ytrrium aluminium garnet from ytrrium and aluminium isobutyrate precursors. *J. Am. Ceram. Soc*., 1996, **79**(2), 385–394.
53. Hay, R. S. Wright Patterson Air Force Base, Dayton, OH; private communication.
54. Heimann, D., Wagner, T., Bill, J., Aldinger, F. and Lange, F. F., Epitaxal growth of β-SiC thin films on a 6H-SiC substrate using the solution precursor method. *J. Mater. Res*., 1997, **12**, 3099–3101.